Article:
Acquaviva, J, He, S, Zhang, C et al. (2014) FGFR3 translocations in bladder cancer: differential sensitivity to HSP90 inhibition based on drug metabolism. Molecular Cancer Research, 12 (7). 1042 - 1054. ISSN: 1541-7786

https://doi.org/10.1158/1541-7786.MCR-14-0004

FGFR3 Translocations in Bladder Cancer: Differential Sensitivity to HSP90 Inhibition Based on Drug Metabolism

Jaime Acquaviva[1], Suqin He[1], Chaohua Zhang[1], John-Paul Jimenez[1], Masazumi Nagai[1], Jim Sang[1], Manuel Sequeira[1], Donald L. Smith[1], Luisa Shin Ogawa[1], Takayo Inoue[1], Noriaki Tatsuta[1], Margaret A. Knowles[2], Richard C. Bates[1], and David A. Proia[1]

[1]Synta Pharmaceuticals Corp., Lexington, Massachusetts; [2]Leeds Institute of Molecular Medicine, St. James's University Hospital, Leeds, United Kingdom.

Running Title: HSP90 inhibition in FGFR3 fusion-positive bladder cancer

Keywords: HSP90 inhibition, bladder cancer, FGFR3, drug metabolism, ganetespib.

Financial Support: All work was funded by Synta Pharmaceuticals Corp.

Corresponding author information: David Proia, Synta Pharmaceuticals Corp., 125 Hartwell Avenue, Lexington, MA 02421. Phone: 781-541-7236; Fax: 781-541-6350; Email: dproia@syntapharma.com

Disclosure of Potential Conflicts of Interest: All authors with the exception of Margaret A. Knowles are current employees of Synta Pharmaceuticals Corp.

Word Count: 6925

Figures/Tables: 8 (6 Figures/2Tables) – After Reviewer request for additional data

Abstract

Activating mutations and/or overexpression of fibroblast growth factor receptor 3 (FGFR3) are commonly observed in bladder cancer, making FGFR3 an attractive therapeutic target in this disease. Recently *FGFR3* gene rearrangements have been described that define a unique subset of bladder tumors. Here we show that the selective heat shock protein 90 (HSP90) inhibitor ganetespib induced loss of FGFR3-TACC3 fusion protein expression and depletion of multiple oncogenic signaling proteins in RT112 bladder cells, resulting in potent cytotoxicity comparable to the pan-FGFR tyrosine kinase inhibitor BGJ398. In contrast to BGJ398, however, ganetespib exerted pleiotropic effects on additional mitogenic and survival pathways and could overcome the FGFR-inhibitor resistant phenotype of FGFR3 mutant-expressing 97-7 and MHG-U3 cells. Combinatorial benefit was observed when ganetespib was used with BGJ398 both *in vitro* and *in vivo*. Interestingly, two additional FGFR3 fusion-positive lines (RT4 and SW480) retained sensitivity to HSP90 inhibitor treatment by the ansamycins 17-AAG and 17-DMAG yet displayed intrinsic resistance to ganetespib or AUY922, both second-generation resorcinol-based compounds. Both lines expressed considerably higher levels of endogenous UGT1A enzyme expression than RT112; this phenotype resulted in the rapid metabolism (via glucuronidation) and subsequent efflux of ganetespib from SW780 cells, thus providing a mechanism to account for the lack of bioactivity.

Implications: These findings suggest that pharmacological blockade of the molecular chaperone HSP90 represents a promising approach for treating bladder tumors driven by oncogenic gene rearrangements of *FGFR3*. Further, UDP-glucuronosyltransferase (UGT) enzyme expression may serve as a predictive factor for clinical response to resorcinol-based HSP90 inhibitors.

Introduction

Bladder cancer represents the fifth most common malignancy worldwide and a major cause of cancer-related morbidity and death. Incidence and mortality rates have remained relatively constant over the past four decades, with an estimated 72,570 new cases and 15,210 deaths predicted for 2013 in the U.S. alone (1). A vast majority of patients, over 70%, present with non-muscle invasive bladder cancer (NMIBC), previously referred to as 'superficial' bladder cancer (2). A proportion (around 10-20%) of these tumors may ultimately progress to invasive disease, but even the bulk percentage of these neoplasms have a characteristically high risk of recurrence which presents an immense challenge for the clinical management and ongoing surveillance of patients, often over many years. The remaining cases are diagnosed as muscle invasive bladder cancer (MIBC), a more aggressive stage of the disease that is associated with a higher risk of metastasis and for which the 5-year survival rates are only around 50% (2). Indeed, progression to metastatic bladder cancer, whether from recurrent NMIBC or MIBC, results in significantly poorer survival outcomes and is generally considered incurable (3). In contrast to other malignancies, advances in the management and treatment of bladder cancer have been limited (4); consequently there exists a considerable unmet need for novel therapeutic approaches to improve patient outcomes in this disease indication.

Fibroblast growth factor receptor 3 (FGFR3) is a member of a structurally related family of tyrosine kinase receptors (FGFR1-4) that orchestrate a diverse variety of cellular activities, including proliferation, differentiation, and survival (5). Ligand binding promotes receptor dimerization, transphosphorylation of key tyrosine residues, and recruitment of adaptor proteins - ultimately leading to the activation of multiple downstream signaling cascades, including PI3K/AKT, RAS/MAPK, STATs, and phospholipase Cγ (PLCγ) (5). Somatic mutation of the *FGFR3* gene is one of the most frequent genetic alterations seen in bladder cancer, occurring in around 75% of all cases of NMIBC (6, 7). Interestingly, most of the missense mutations identified in bladder tumors are identical to germline gain-of-function mutations responsible for autosomal dominant human skeletal disorders and dwarfism syndromes (5, 8). *FGFR3* mutations are less prevalent in muscle-invasive tumors, which more commonly exhibit dysregulated FGFR3 function via overexpression of the wild-type protein (7). Recently, a third mechanism of aberrant FGFR3 activation in

bladder cancer has been identified that involves chromosomal rearrangements of *FGFR3* with one of two different fusion partners: *TACC3* (transforming acid coiled coil 3) or *BAI1AP2L1* (BAI1-associated protein 2-like 1) (9). Both *FGFR3-TACC3* and *FGFR3-BAI1AP2L1* translocations generate constitutively activated and oncogenic FGFR3 kinase protein products, and cellular dependence on these drivers confers sensitivity to selective FGFR inhibition (9, 10). In light of these and other considerations, FGFR3 has long been considered an attractive actionable target for novel therapeutic approaches in bladder cancer (11).

The molecular chaperone heat shock protein 90 (HSP90) plays an essential role in regulating the maturation and functional stability of an extensive array of cellular client proteins, an activity that is often exploited by cancer cells to confer aberrant proliferative, survival, and/or metastatic potential (12, 13). Indeed the HSP90 machinery serves as a biochemical buffer for a number of oncogenic signaling proteins that have been causally implicated in a variety of human tumors; mutant oncoproteins have been shown to be particularly reliant on the chaperone (14, 15). Functional inhibition of HSP90 results in the simultaneous degradation of hundreds of clients; thus providing a mechanism to concomitantly disrupt multiple oncogenic signaling cascades through a singular molecular target. In this regard, pharmacological blockade of HSP90 has emerged as an innovative approach for the development of new antineoplastic agents (16).

We have previously shown that selective targeting of HSP90 activity using ganetespib, a potent small molecule inhibitor of HSP90 (17), represents a valid and superior alternative approach to direct kinase inhibition in EML4-ALK fusion protein-driven lung cancer (18). Here we report on our evaluation of this strategy in FGFR3 fusion-positive bladder cancer cells. Ganetespib activity was examined in a panel of bladder lines to determine the comparative sensitivity of *FGFR3*-rearranged cells to this treatment modality. Additionally we explored the efficacy of combinatorial ganetespib plus FGFR inhibitor treatment as a means to optimize the antitumor potency of HSP90 blockade. Significantly, FGFR3 fusion-driven bladder cells showed differential sensitivity to alternate chemical classes of HSP90 inhibitors irrespective of the translocation present; and a series of studies were performed to dissect the underlying basis of this response. Overall, the results suggest that selective inhibition of HSP90 represents a new therapeutic opportunity to target bladder cancer cells driven by oncogenic rearrangements of FGFR3. Moreover, the

data identify additional molecular markers that may be indicative of intrinsic resistance to specific classes of small molecule HSP90 inhibitors, a finding with important translational implications for the potential clinical application of these drugs in bladder cancer.

Materials and Methods

Cell lines, antibodies, and reagents

The RT4 and SW780 cell lines were obtained from the American Type Culture Collection (ATCC). Each was maintained according to suppliers' instructions, authenticated by routine company DNA typing, and used within six months of receipt. RT112 cells were obtained from Sigma-Aldrich. The 97-7 and MGH-U3 lines are established in the Knowles laboratory and cell line identity was verified by short tandem repeat DNA typing using a Powerplex 16 kit (Promega). The remaining fifteen bladder lines listed in Table 1 are part of a collection assembled by the Center for Molecular Therapeutics (Massachusetts General Hospital Cancer Center) who performed the drug sensitivity analysis. As part of the establishment of this cell line collection, a panel of 92 SNPs (single nucleotide polymorphisms) was profiled for each cell line and short tandem repeat analysis was also performed. All primary antibodies were purchased from Cell Signaling Technology with the exception of the FGFR3 (B9) and glyceraldehyde-3-phosphate dehydrogenase (GAPDH) antibodies (Santa Cruz Biotechnology, Inc.), UGT1A9 (Abcam), and UGT1A10 (Novus Biologicals). Ganetespib [3-(2,4-dihydroxy-5-isopropylphenyl)-4-(1-methyl-1H-1,2,4-triazol-5(4H)-one] was synthesized by Synta Pharmaceuticals Corp. 17-AAG and 17-DMAG were purchased from LC Laboratories; BGJ398 and AUY922 from Selleck Chemicals; and propofol from Sigma Aldrich.

Viability assays

Cellular viability was assessed using the CellTiter-Glo Luminescent Cell Viability Assay (Promega) according to manufacturer protocols. Bladder cancer cell lines were seeded into 96-well plates based on optimal growth rates determined empirically for each line. All viability assays were performed in triplicate. Twenty-four hours after plating, cells were dosed with graded concentrations of ganetespib for 72 hours. CellTiter-Glo was added (50% v/v) to the cells, and the plates incubated for 10 minutes prior to luminescent detection in a SpectraMax Plus 384 microplate reader (Molecular Devices). Data were normalized to percent of control and IC_{50} values used to determine the sensitivity of each line. For the comparative analyses with ganetespib and BGJ398, RT112 cells were treated with graded concentrations of each compound for 72 hours and cell viability measured as above. For the evaluation of apoptotic

induction, caspase activity was assessed using the Caspase-Glo 3/7 assay (Promega) according to manufacturer protocols. Twenty-four hours after plating, RT112 cells were treated with graded concentrations of ganetespib for 24 hours. Caspase-Glo was added to cells (50% v/v) and the plates incubated for 1 hour prior to luminescent detection.

Western blotting

Following *in vitro* assays, tumor cells were disrupted in lysis buffer on ice for 10 minutes. Lysates were clarified by centrifugation and equal amounts of proteins resolved by SDS-PAGE before transfer to nitrocellulose membranes (Bio-Rad). Membranes were blocked with StartingBlock T20 blocking buffer (Thermo Scientific) and immunoblotted with the indicated antibodies. Antibody-antigen complexes were visualized using an Odyssey system (LI-COR).

Reverse phase protein array

RT112 cells were treated with dimethyl sulfoxide (DMSO, control) or 100 nM ganetespib for 24 hours. Lysates were prepared as recommended by MD Anderson Cancer Center (Houston, TX) with cellular proteins denatured by 1% SDS (with beta-mercaptoethanol) and diluted in five 2-fold serial dilutions in dilution buffer (lysis buffer containing 1% SDS). Serial diluted lysates were arrayed on nitrocellulose-coated slides (Grace Biolab) by an Aushon 2470 Arrayer (Aushon BioSystems). A total of 5808 array spots were arranged on each slide including the spots corresponding to positive and negative controls prepared from mixed cell lysates or dilution buffer, respectively. Each slide was probed with a validated primary antibody plus a biotin-conjugated secondary antibody (19). Only antibodies with a Pearson correlation coefficient between RPPA and western blotting of greater than 0.7 were used in reverse phase protein array analysis. The signal obtained was amplified using a Dako Cytomation–catalyzed system (Dako) and visualized by DAB colorimetric reaction. The slides were scanned, analyzed, and quantified using Microvigene software (VigeneTech Inc.) to generate spot intensity.

Each dilution curve was fitted with a logistic model developed by the Department of Bioinformatics and Computational Biology (MD Anderson Cancer Center). The fitted curve is plotted with the signal intensities – both observed and fitted - on the y-axis and the $\log_2$-concentration of proteins on the x-axis

for diagnostic purposes. The protein concentrations of each set of slides were normalized by median polish, which was corrected across samples by the linear expression values using the median expression levels of all antibody experiments to calculate a loading correction factor for each sample.

In vivo xenograft tumor models

CD-1 nude mice (Charles River Laboratories, Wilmington, MA) at 7-12 weeks of age were maintained in a pathogen-free environment and all *in vivo* procedures were approved by the Synta Pharmaceuticals Corp. Institutional Animal Care and Use Committee. RT112 cells ($5x10^6$) were subcutaneously implanted into female mice and animals bearing established tumors (~150 mm^3) were randomized into treatment groups of 8. Mice were i.v. dosed with ganetespib (150 mg/kg) once weekly or p.o. dosed with BGJ398 (10 mg/kg) daily, either alone or in combination, for 3 weeks. Tumor growth inhibition was monitored by tumor volume measurements twice weekly. As a measurement of *in vivo* efficacy, the %T/C value was determined from the change in average tumor volumes of each treated group relative to the vehicle-treated animals. Statistical significance was determined using two-way ANOVA followed by Bonferroni post tests.

Pharmacodynamics

Nude mice bearing established RT112 xenografts were randomized into groups of 3 and administered a single bolus injection of ganetespib (150 mg/kg) or vehicle. At 24 and 72 hours post treatment, tumors were resected and homogenized in lysis buffer. Expression changes in cell signaling pathway components were interrogated using Pathscan RTK Signaling and Pathscan Intracellular Signaling Array Kits (Cell Signaling Technology) according to manufacturer protocols. Fluorescence readouts were measured using an Odyssey system (LI-COR) and average changes in signaling protein expression were calculated for each cohort.

Bioanalysis

In the first set of experiments, RT112 and SW780 cells were treated with graded concentrations of ganetespib or 17-DMAG (10-1000 nM) for 1 and 24 hours. Cell lysates were prepared for measurement of intracellular concentrations of the respective HSP90 inhibitors. RT112 and SW780 cells were also

treated with 1 μM ganetespib for 15 minutes, 1, 4, 8 and 24 hours. At each time point cell lysates were prepared and media was collected for analysis of intracellular and secreted concentrations of ganetespib and its glucuronidated metabolites. Bioanalysis was performed on equal protein concentrations from cell lysates or equal volumes of media. All samples were ultimately extracted by protein precipitation and analyzed by LC-MS/MS using an Agilent 1100 HPLC interfaced to an API 4000 tandem mass spectrometer (Applied Biosystems). A Phenomenex Kinetex 2.6μm C18 (30 x 2.1 mm) column was used with a run time of 3.5 min per sample.

UGT1A gene expression analysis

Total RNA was extracted from untreated SW780 and RT112 cells using the RNeasy Kit (Qiagen Inc.). cDNA (1 μg) was synthesized using an iScript cDNA synthesis kit (Bio-Rad). RT-PCR was performed using custom primers for UGT1A1, UGT1A3, UGT1A4, UGT1A5, UGT1A6, UGT1A7, UGT1A8, UGT1A9, and UGT1A10 (Bio-Rad). The cycling conditions were 95^{o} C for 2 minutes, followed by 40 cycles of 95^{o} for 10 seconds and 60^{o} for 30 seconds. Data were normalized to two housekeeping genes (hypoxanthine phosphoribosyltransferase 1 [HPRT1] and glyceraldehyde-3-phosphate dehydrogenase [GAPDH]) and analyzed by comparing $2^{-\Delta Ct}$ of the normalized sample. PCR was performed on a Bio-Rad iCycler iQ5 (Bio-Rad).

siRNA knockdown assay

The Nucleofector® transfection system (Lonza) was used for cell transfections using standard manufacturer protocols. Briefly, for each siRNA construct 3-5 $x10^{5}$ SW780 cells resuspended in 100 μl supplemented nucleofector solution were transiently transfected with siRNA-negative control or 300 nM siRNA-UGT1A7,8,9,10 mix (30 pmol/sample, Invitrogen). Transfected cells were grown for 72 hours. Cell cultures were then exposed to graded concentrations of ganetespib (0, 100, 1000 nM) for 24 hours prior to lysis and analysis by Western blot.

Competitive UGT1A9 inhibitor assay

SW780 cells were cultured with 0.5 μM ganetespib, 100 μM and 300 μM propofol, both alone and in combination, or vehicle (DMSO) for 24 hours. At the end of the incubation, cells were harvested, lysed and protein expression changes evaluated by Western blot.

Results

Ganetespib displays potent cytotoxic activity in FGFR3-driven bladder cancer lines

Sensitivity to targeted HSP90 inhibition by ganetespib was evaluated using a panel of 20 bladder cancer cell lines of diverse genetic FGFR3 backgrounds (Table 1). In the majority of lines examined ganetespib reduced cellular viability with low nanomolar potency, including all that expressed activating point mutations. Further, ganetespib treatment could overcome an intrinsic FGFR inhibitor-resistant phenotype displayed by mutant FGFR3-expressing 97-7 and MGH-U3 cells (Supplementary Fig. S1). These lines harbor $FGFR3^{S249C}$ and $FGFR3^{Y375C}$ mutations, respectively, and were insensitive to the pan-FGFR inhibitor BGJ398 yet both remained susceptible to the cytotoxic effects of ganetespib exposure (Supplementary Fig. S1).

Suppression of multiple oncogenic signaling cascades in FGFR3 fusion-driven RT112 bladder cancer cells by ganetespib

From the initial analysis, RT112 cells were found to be acutely sensitive to ganetespib treatment (IC_{50} value 9 nM, Table 1). Long considered over-expressers of wild type FGFR3, the recent identification of the *FGFR3-TACC3* fusion gene product in these cells accounts for their critical dependence on FGFR3 activity for growth and survival (9). Moreover, bladder cell lines now known to be FGFR3 fusion-positive, including RT112, have been reported to be highly sensitive to BGJ398 (20). In this regard, ganetespib was equipotent to selective FGFR inhibition in reducing cell viability in this line (Fig. 1A). This loss of viability was concurrent with activation of apoptosis as shown in Fig. 1B. RT112 cells were exposed to increasing concentrations of ganetespib and viability measured at 72 hours. This profile was compared to apoptotic induction determined by activated caspase 3/7 levels assessed 24 hours post treatment, which showed that ganetespib-induced cytotoxicity was mediated by an irreversible commitment to apoptosis.

Next we examined molecular changes in client and signaling protein pathways associated with FGFR3-TACC3 in ganetespib-treated RT112 cells (Fig. 1C). Ganetespib induced a robust and dose-dependent destabilization of FGFR3-TACC3 expression, in terms of both total and phosphorylated protein levels, suggesting that the FGFR3 fusion protein was highly responsive to HSP90 inhibition. Importantly,

targeted degradation of this oncogenic driver was accompanied by loss of downstream signaling effector activity (as evidenced by loss of phosphorylated ERK and AKT levels) and induction of BIM, an additional marker of apoptosis (Fig. 1C). Consistent with its alternative mode of action as a specific tyrosine kinase inhibitor, an effective dose of BGJ398 (100 nM) did not affect total FGFR3-TACC3 expression but resulted in a similar abrogation of autophosphorylated FGFR3-TACC3 activity, disruption of oncogenic pathways, and induction of apoptosis. When the kinetics of client protein loss in response to HSP90 inhibition were examined (Fig. 1D), it was found that destabilization of the FGFR3-TACC3 fusion and the congruent alterations in downstream signaling were relatively rapid, occurring within 4 hours of ganetespib exposure. Indeed, the destabilization profile for the FGFR3-TACC3 protein was similar to that of HER2, a highly sensitive HSP90 client.

A feature of targeted HSP90 blockade is the simultaneous disruption of multiple cellular signaling cascades and processes that are exquisitely dependent on the chaperoning function of the molecule. Therefore we performed a more extensive reverse phase protein array analysis of ganetespib effects in RT112 cells. In addition to the expected downregulation of client receptor tyrosine kinases such as HER2, MET and EGFR, ganetespib treatment also selectively altered the expression of a number of proteins involved in mitogen-activated protein kinase (MAPK), AKT, and mammalian target of rapamycin (mTOR) signaling and cell cycle regulation, along with predicted increases in the apoptotic markers caspase 7 and BIM (Table 2). Thus, the potent and selective disruption of FGFR3-mediated signaling coupled with coordinate effects on additional mitogenic and survival pathways in RT112 cells accounts for the potent cytotoxic activity of ganetespib in this line.

Ganetespib in combination with FGFR3 tyrosine kinase inhibition confers superior antitumor activity *in vitro* and *in vivo*

Based on their distinct mechanisms of action on FGFR3-TACC inhibition, we examined whether combining ganetespib and BGJ398 would lead to increased activity in FGFR3 fusion-dependent bladder cancer cells. To do this, we first evaluated the effects on cellular viability following combination exposure in the RT112 cell line (Fig. 2A). The bladder cancer cells were treated with increasing concentrations of ganetespib and/or BGJ398 and viability assessed after 72 hours. The percentages represent the degree

of cell death at each individual dose level, which revealed that combinatorial benefit was achieved at all concentrations tested. For example, at the approximate IC_{50} concentrations for each inhibitor (9.6 nM for ganetespib and 5 nM for BGJ398), combined exposure resulted in 71% cell killing. Overall, all combinations of ganetespib and BGJ398 showed improved cell killing activity over single-agent treatment alone.

To determine whether these effects on cell viability *in vitro* would translate to improved efficacy *in vivo*, RT112 xenograft bearing mice were treated with ganetespib and BGJ398, both as single agents and in combination. We have previously determined that the maximally tolerated dose of ganetespib on a weekly dosing regimen is 150 mg/kg (17). Weekly administration of ganetespib at this dosing level was comparable to daily dosing of BGJ398 at 10 mg/kg, with each compound inducing a similar degree of tumor regression (T/C values of -23% and -20%, respectively; Fig. 2B). Concurrent treatment with both drugs resulted in a significant enhancement of antitumor activity, causing 66% tumor regression. In addition, combination treatment was well tolerated, with no significant changes in body weights seen after 3 weeks of treatment (data not shown). Thus, ganetespib and BGJ398, when combined, displayed superior antitumor efficacy compared to monotherapy in RT112 bladder tumor xenografts.

Next pharmacodynamic analysis was performed in additional mice bearing RT112 xenografts to confirm that the ganetespib-induced tumor response correlated with target modulation *in vivo*. Animals were treated with a bolus injection of ganetespib at 150 mg/kg and tumors harvested 24 and 72 hours later. Control group mice were administered a single injection of vehicle and tumors excised at the same time points. Expression changes in components of multiple signaling pathways, including receptor tyrosine kinases and their effector proteins, were investigated using multiplexed antibody arrays; average changes for each treatment cohort are presented in Fig. 2C. Ganetespib exposure resulted in the deactivation of endogenous FGFR3-TACC3 activity, as evidenced by the significant repression of p-FGFR3 levels and congruent repression of phosphorylated ERK and AKT by 24 hours. These effects were sustained over time with recovery occurring at 72 hours post treatment. Similar kinetics were observed for signaling intermediates of the mTOR pathway (phosphorylated S6 ribosomal protein and PRAS40), consistent with what was observed following targeted HSP90 inhibition *in vitro* (Table 2). Overall, these data show that

single-dose ganetespib exerts a potent and rapid destabilizing effect on the FGFR3-TACC3 fusion kinase and its effectors in RT112 xenografts.

Differential sensitivity of FGFR3 fusion-positive bladder cancer lines to HSP90 inhibitors

As part of a previous study it was shown that RT112 and RT4 bladder cancer cells, which also express the FGFR3-TACC3 fusion protein, were sensitive to targeted HSP90 inhibition by the first-generation ansamycin compound 17-AAG (17-allylamino-17-demethoxygeldanamycin) (21). However, RT4 cells were largely insensitive to ganetespib exposure (Table 1). To explore this lack of activity with ganetespib we evaluated the cytotoxicity of four HSP90 inhibitors (HSP90i) in RT4 and SW780 cells: 17-AAG, the closely related ansamycin analog 17-DMAG (17-dimethylaminoethylamino-17- demethoxygeldanamycin), ganetespib, and another resorcinol-based second-generation inhibitor AUY922 (Fig. 3A). In RT4 cells, exposure to an ansamycin-based HSP90i resulted in dose-dependent cytotoxicity and low nanomolar IC_{50} values. In contrast, ganetespib and AUY922 were minimally effective at reducing cellular viability with IC_{50} values greater than 1 μM (Fig. 3A).

At the molecular level, 17-DMAG and 17-AAG both effectively destabilized FGFR3 and higher weight FGFR3-TACC3 fusion protein expression in RT4 cells (Fig. 3B). This was accompanied by a concomitant loss of downstream ERK activity (Fig. 3C). In addition, two other sensitive HSP90 client proteins, HER2 and CDC2, were similarly degraded in a concentration-dependent manner. Consistent with the viability results, a corresponding dose-dependent increase in BIM expression was observed supporting the premise that both of these first-generation HSP90i induced apoptosis in RT4 cells (Fig. 3C). As predicted by the sensitivity profile of this line, ganetespib had negligible effects on the expression of any of the same molecular markers (Fig. 3D).

This pattern was repeated in the SW780 line which harbors an *FGFR3-BAI1AP2L1* gene rearrangement. The two resorcinol-based inhibitors were again only weakly cytotoxic yet the cells remained acutely sensitive to 17-AAG and 17-DMAG treatment (Fig. 4A). In stark contrast to 17-AAG, neither ganetespib nor AUY922 were found to significantly affect FGFR3-BAI1AP2L1 fusion protein levels, wild-type FGFR3, downstream effector pathways (p-ERK, p-AKT), or other established HSP90 client proteins (MET, HER2)

(Fig. 4B). These data were additionally supported by the dose-dependent analysis of ganetespib activity shown in Fig. 4C. No changes in FGFR3-BAI1AP2L1, phosphorylated FGFR3, ERK, AKT or MEK, or MET levels were observed, suggesting that the HSP90 inhibitory activity of the compound was compromised in this cell line. Taken together, these data show that the *FGFR3-TACC3* and *FGFR3-BAI1AP2L1* gene fusion products were sensitive HSP90 client proteins, as evidenced by the potent effects of 17-AAG and 17-DMAG on protein destabilization and cell viability in RT4 and SW780 cells, respectively. However, the lack of client protein modulation and cytotoxic activity seen with ganetespib and AUY922 suggested that these two cell lines exhibited an intrinsic level of resistance to the resorcinol-based, second-generation HSP90i.

High expression of UGT1A enzyme expression in FGFR3 fusion-positive bladder cells results in glucuronidation and efflux of ganetespib

To dissect the mechanisms underlying the differential sensitivities to specific HSP90i exhibited by the FGFR3 fusion-positive cell lines, we first compared the intracellular concentrations of ganetespib and 17-DMAG in the 'resorcinol-sensitive' RT112 and 'resorcinol-resistant' SW780 cell lines as a function of time (Fig. 4A). In RT112 cells, both compounds accumulated in a dose-dependent manner 1 hour post treatment, albeit with comparatively higher total ganetespib levels than 17-DMAG at each concentration tested. Moreover, the intracellular levels for each HSP90i seen after 1 hour appeared to approach saturation since no significant increases were observed at the 24-hour time point (Fig. 5A, *left panel*). In the SW780 cell line, the initial accumulations of ganetespib and 17-DMAG were indistinguishable, with each HSP90i readily entering and accumulating to near identical concentrations at 1 hour. By 24 hours, levels of 17-DMAG were maintained and modestly increased; in stark contrast virtually no ganetespib was detectable within the intracellular compartment of SW780 (Fig. 5A, *right panel*).

These data suggested that ganetespib resistance was not due to differences in HSP90 biology but likely attributable to drug efflux and/or metabolism mechanisms. Similar to AUY922 (22), ganetespib is susceptible to metabolism by the UGT1A family of UDP-glucuronosyltransferase enzymes that transform small lipophilic molecules into water-soluble, excretable metabolites (23). Therefore the intracellular and secreted levels of ganetespib and its glucuronidated metabolites were measured in RT112 and SW780

cells as a function of time (Fig. 5B). No glucuronidated form of ganetespib was detectable within RT112 cells over a 24-hour time course and only a minor concentration of metabolites was observed in the culture medium at the last time point (Fig. 5B, *left panel*). Notably, approximately 40% of the total intracellular drug levels present in the SW780 line 15 minutes following drug addition were glucuronidated compounds (Fig. 5B, *right panel*), indicating that ganetespib was being rapidly metabolized in these cells. In agreement with the data shown in Fig. 5A, intracellular SW780 ganetespib concentrations decreased to undetectable levels by 24 hours; this was concomitant with a marked accumulation of metabolite secretion into the culture media with time (Fig. 5B, *right panel*).

When overall UGT1A protein expression was evaluated in the three FGFR3 fusion-positive bladder lines it was found that both SW780 and RT4 cells expressed considerably higher endogenous enzyme levels compared to RT112 (Fig. 5C). Further, UGT1A protein expression was virtually undetectable in 97-7 bladder cancer cells, which were also sensitive to ganetespib exposure (Supplementary Fig. S1). We subsequently performed a comparative PCR analysis assessing relative mRNA levels of individual UGT1A family enzymes to examine differences in metabolism-related gene expression between the RT112 and SW780 cell lines (Fig. 5D). From this screen it was found that SW780 cells showed significantly higher basal UGT1A family expression compared to the RT112 line, most notably the *UGT1A7*, *UGT1A8*, *UGT1A9*, and *UGT1A10* isoforms – which represent a cluster of genes encoding highly homologous enzymes within the UGT1A subfamily (24). Of note, we have previously identified UGT1A9 as the primary UGT enzyme responsible for ganetespib glucuronidation in liver microsome assays (data not shown). To confirm the PCR findings, UGT1A9 and 1A10 protein expression were individually evaluated in the panel of lines, with UGT1A9- and UGT1A10-tranfected 293T cells serving as a positive control (Fig. 5E). As predicted, the SW780 and RT4 cell lines expressed considerably higher endogenous levels of both enzymes compared to RT112 cells. These data indicated that of the three FGFR3 fusion-positive lines, SW780 and RT4 cells had a higher intrinsic propensity to metabolize ganetespib than RT112, and suggested that this phenotypic variation contributed to the differential sensitivities seen following drug exposure. Taken together, our findings support the premise that high endogenous UGT1A enzyme expression in SW780 cells promoted the rapid glucuronidation and subsequent efflux of ganetespib, sufficient to account for its lack of bioactivity in this line.

Targeted reductions in UGT1A activity by RNA interference or competitive inhibition sensitize SW780 bladder cells to ganetespib

To confirm this putative mechanism of action, we performed a series of reversion experiments in SW780 bladder cells. In the first, UGT expression was modulated by transfecting SW780 cells with a non-target (control) or UGT1A7,8,9,10-targeting siRNA probe for 72 hours. HSP90 inhibitory activity was then compared in control and UGT1A-deficient SW780 cells exposed to increasing concentrations of ganetespib for a further 24 hour period (Fig. 6A). Immunoblotting revealed that targeted RNA interference effectively resulted in the complete abrogation of UGT1A9 and UGT1A10 protein expression. Upregulation of heat shock protein 70 (HSP70) was used as a surrogate marker of HSP90 inhibition (25) and effects on two well-established client proteins, epidermal growth factor receptor (EGFR) and cyclin-dependent kinase 1 (CDK1), were assayed. Control cells were largely insensitive to the effects of ganetespib exposure, reflecting the phenotype of the parental SW780 line. In stark contrast, UGT1A9/1A10-deficient SW780 cells showed marked increases in HSP70 expression, alongside dose-dependent destabilization of both EGFR and CDK1. Moreover, ganetespib treatment at the highest dose resulted in the induction of apoptosis, as evidenced by cleaved PARP expression. Taken together, these data showed that siRNA knockdown of UGT1A9 and 1A10 expression could overcome intrinsic ganetespib resistance in SW780 bladder cells.

Reductions in glucuronidation activity were also assessed by treating SW780 cells with ganetespib in the presence or absence of propofol, a competitive inhibitor of UGT1A9 activity (26). As expected, ganetespib treatment alone had only minor effects on HSP70 induction and client protein stability; propofol exposure (100 and 300 μM concentrations) exhibited no discernable effects on HSP90 activity (Fig. 6B). However, in the presence of propofol, SW780 cells were sensitized to ganetespib treatment as shown by robust HSP70 upregulation, more complete degradation of both client proteins, and marked elevations in cleaved PARP levels. Together with the siRNA data, these observations provide further support for glucuronidation-based metabolism as representing the primary mechanism of ganetespib resistance in this bladder model.

Finally, we reasoned that the differences in metabolic profiles exhibited by the FGFR3-fusion positive bladder cancer lines may also confer differential sensitivity to a wider variety of therapeutic agents, in addition to HSP90i. To examine this possibility, we interrogated the Genomics of Drug Sensitivity in Cancer Project database (http://www.cancerrxgene.org). Clinically validated, targeted compounds that showed 3-fold or higher changes in IC_{50} cytotoxicity values for SW780 cells compared to the RT112 line are listed in Supplementary Table S1. In agreement with the findings shown in Fig. 4A, NVP-AUY922 was identified in the screen, as was another resorcinol-based HSP90i CCT018159. In general terms, targeted agents that exhibited the highest potential for Phase II/glucuronidation metabolism were associated with higher IC_{50} ratios, indicating that SW780 cells were far less sensitive to drug treatment than RT112. Overall, these data suggest that metabolism-based resistance linked to UGT1A expression may represent a more general consideration for the evaluation of variety of anticancer compounds in bladder tumors.

Discussion

FGFR3 has long been considered an attractive therapeutic target in bladder cancer based on its high frequency of dysregulated activity, particularly through mutation and/or over-expression (11). Importantly, FGFR3 has been implicated to play a key oncogenic role in both non-invasive and invasive disease (7). The recent discovery of genomic *FGFR3* rearrangements in a subset of bladder tumors provides another pathogenic mechanism for aberrant FGFR3 activation in this disease and one with particular relevance for the identification of patients who may ultimately benefit from targeted FGFR inhibition (9). The fusion gene products generated by rearrangements of *FGFR3* with either *TACC3* or *BAI1AP2L1* are tumorigenic and create dependency in cell lines harboring such alterations (9, 10). Moreover, transforming fusions of *FGFR* and *TACC* genes have also been found in glioblastoma (27), suggesting that translocation may represent a more universal mechanism of FGFR dysregulation that is conserved across tumor types. Of note, constitutively active fusion gene products are well characterized as critical driver proteins in other cancer types, such as *EML4-ALK* in non-small cell lung cancer and *BCR-ABL* in chronic myeloid leukemia (28-30). Indeed, the clinical successes of agents directed against such proteins (e.g., crizotinib for EML4-ALK and imatinib for BCR-ABL) have served as paradigms for the design and application of molecularly targeted therapy in cancer. A number of small molecules with activity against FGFRs are currently under development, the majority of which are multi-kinase inhibitors originally designed as antiangiogenic agents against other growth factor receptors (31). Recently, more selective and potent pan-FGFR inhibitors, including BGJ398 (20), have entered early stage clinical evaluation in bladder and other tumor types (31).

In this report we show that bladder cancer cell lines harboring *FGFR3-TACC3* and *FGFR3-BAI1AP2L1* gene rearrangements are sensitive to HSP90 inhibition. Previously, 17-AAG has been reported to exert *in vitro* cytotoxic activity in RT112 and RT4 cells (21), however the presence and significance of the *FGFR3-TACC3* product expressed in these lines were not recognized in that study. Here we provide the first demonstration that FGFR3 fusion proteins expressed by bladder cancer cells are reliant on the chaperoning activity of the HSP90 molecule for their stability and function, as evidenced by their pronounced destabilization following HSP90i treatment (in an inhibitor-dependent context), ultimately

leading to loss of tumor cell viability. While this finding alone does not unequivocally identify FGFR3 fusions as direct HSP90 substrates, it is important to note that the FGFR3 kinase itself is a *bona fide* HSP90 client protein (32, 33). Indeed, within the FGFR family of receptor tyrosine kinases there is a hierarchical degree of destabilization induced by selective HSP90 inhibitors, with FGFR3 representing the member most sensitive to chaperone inhibition (33). In RT112 cells, ganetespib exposure resulted in the rapid and potent degradation of FGFR3-TACC3 protein expression, loss of downstream effector signaling, and subsequent induction of apoptosis. HSP90 blockade was as effective as direct kinase inhibition afforded by BGJ398 treatment and, importantly, the *in vitro* antitumor activity of both compounds was recapitulated *in vivo*. BGJ398 administration induced tumor regressions in *FGFR3-TACC3*-driven RT112 xenografts - a response that was both consistent with, and superior to, what has been observed with the small molecule FGFR kinase inhibitor PD173074 in RT4 and SW780 models (10). A weekly dosing schedule of ganetespib was equally efficacious as the BGJ398 regimen. We extended these findings by combining the two modalities of HSP90 inhibition and selective FGFR3 targeting in RT112 tumors, which resulted in improved efficacy over that achieved with either agent alone. Together with the broader spectrum of biological activity conferred by ganetespib exposure, these data strongly suggest that HSP90 inhibition offers an alternative, and potentially complementary, strategy to selective kinase inhibition in FGFR3 fusion-driven bladder cancer.

An interesting feature of FGFR fusion-positive tumor lines is their enhanced susceptibility to pharmacologic inhibition by selective FGFR kinase inhibitors over activating point mutations (10). In this regard, ganetespib retained full potency against two BGJ398-resistant bladder cell lines, 97-7 and MGH-U3, which bear mutant $FGFR3^{S249C}$ and $FGFR3^{Y375C}$ receptors, respectively. Further, ganetespib was also highly potent in reducing cell viability in a number of bladder cell lines with wild type FGFR3 status – highlighting the therapeutic potential of pharmacological HSP90 blockade for affecting this validated and actionable disease target. Clinically, the field of FGFR-targeted therapy is still in its infancy and the translational benefit of any specific agent is yet to be realized. However a recurring theme in the clinical experience with many targeted kinase inhibitor drugs, including imatinib and crizotinib, is that their long-term efficacy is often hampered by the invariable development of acquired resistance, commonly arising due to the acquisition of secondary mutations in their respective kinase targets (34, 35). We and others

have previously shown that HSP90 inhibition is an effective approach for overcoming oncogenic EML4-ALK activity in non-small cell lung cancer (18, 36, 37). Significantly, ganetespib also displayed potent activity against a variety of acquired ALK mutations that confer crizotinib resistance in multiple experimental models and in the clinical setting (18). In light of the broader activity profile of ganetespib in affecting both activating mutations and translocations of FGFR3, it is reasonable to suggest that HSP90 blockade may warrant further investigation as a means to overcome acquired resistance should similar mechanisms arise that allow escape from targeted FGFR agents.

A significant finding of this study was the differential sensitivities exhibited by the fusion-positive bladder lines to alternate classes of HSP90 inhibitors. In particular, cell fate following HSP90i exposure in RT4 and SW780 cells varied according to the chemical class of inhibitor used. Both of the first-generation ansamycin inhibitors 17-AAG and 17-DMAG potently induced cell death, and loss of viability was associated with destabilization of the individual FGFR3 fusions expressed by each line. However, and in contrast to RT112 cells, both lines were largely resistant to ganetespib treatment or exposure to AUY922, a second resorcinol-based HSP90i. Mechanistically, the rapid metabolism (via glucuronidation) and subsequent efflux of ganetespib from SW780 cells was sufficient to account for the lack of HSP90 inhibitory activity. This was validated by inhibiting the high endogenous levels of UGT1A9 and UGT1A10 expression in SW780 by RNA interference, as well as competitive inhibition of the UGT1A9 isoform by propofol. Both experimental strategies overcame the intrinsically resistant phenotype of this bladder line, and conferred sensitivity to ganetespib exposure. This is the first demonstration of ganetespib metabolism as a contributing factor to drug resistance and thus has clear implications for the clinical application of the compound. Overall, response to the second-generation resorcinol inhibitors appeared intimately linked to the endogenous level of UGT1A family enzyme expression, the primary catalysts of glucuronidation reactions in multiple human tissues (23). Interestingly, the *UGT1A* gene cluster has been identified as a novel susceptibility locus for bladder cancer using genome-wide association studies (38). Further, experimental evidence has shown that UGT1A expression becomes down-regulated during bladder cancer progression in animal models (39), consistent with the hypothesis that UGT variants mapping to this region may provide a protective, tumor-suppressive function in bladder cells (40). FGFR3 fusion protein expression is likely to be an important biomarker to aid in patient selection when evaluating novel

bladder cancer treatments, due to an increased susceptibility of fusion-bearing tumor cells to targeted FGFR therapies (9). Based on the findings presented here, UGT1A expression in bladder tumors may represent an additional marker with direct translational relevance for the clinical evaluation of HSP90 inhibitor-based strategies. Moreover, we have observed high levels of UGT1A in subsets of lung cancer patients (D. Proia, unpublished observations). Combining these results with patient responses in ongoing clinical trials of ganetespib may be informative as to the potential use of UGT1A as a predictive biomarker for future studies.

In summary, this study provides preclinical proof of concept that targeting FGFR3 gene fusions via selective HSP90 inhibition represents a rational therapeutic strategy for bladder tumors oncogenically driven by this mechanism of aberrant receptor activation. Based on select advantages of this approach over FGFR-specific kinase inhibitors, these findings are likely to provide a framework for the development of new targeted agents and biomarkers designed to improve therapeutic outcomes for bladder cancer patients.

Acknowledgments

We wish to thank Dinesh Chimmanamada for his expert assistance with the compound glucuronidation profiling.

References

1. Siegel R, Naishadham D, Jemal A. Cancer statistics, 2013. CA Cancer J Clin 2013;63:11-30.

2. Kaufman DS, Shipley WU, Feldman AS. Bladder cancer. Lancet 2009;374:239-49.

3. Bellmunt J, Petrylak DP. New therapeutic challenges in advanced bladder cancer. Semin Oncol 2012;39:598-607.

4. Bambury RM, Rosenberg JE. Advanced Urothelial Carcinoma: Overcoming Treatment Resistance through Novel Treatment Approaches. Front Pharmacol 2013;4:3.

5. Turner N, Grose R. Fibroblast growth factor signalling: from development to cancer. Nat Rev Cancer 2010;10:116-29.

6. Billerey C, Chopin D, Aubriot-Lorton MH, Ricol D, Gil Diez de Medina S, Van Rhijn B, et al. Frequent FGFR3 mutations in papillary non-invasive bladder (pTa) tumors. Am J Pathol 2001;158:1955-9.

7. Tomlinson DC, Baldo O, Harnden P, Knowles MA. FGFR3 protein expression and its relationship to mutation status and prognostic variables in bladder cancer. J Pathol 2007;213:91-8.

8. van Rhijn BW, van Tilborg AA, Lurkin I, Bonaventure J, de Vries A, Thiery JP, et al. Novel fibroblast growth factor receptor 3 (FGFR3) mutations in bladder cancer previously identified in non-lethal skeletal disorders. Eur J Hum Genet 2002;10:819-24.

9. Williams SV, Hurst CD, Knowles MA. Oncogenic FGFR3 gene fusions in bladder cancer. Hum Mol Genet 2013;22:795-803.

10. Wu YM, Su F, Kalyana-Sundaram S, Khazanov N, Ateeq B, Cao X, et al. Identification of targetable FGFR gene fusions in diverse cancers. Cancer Discov 2013;3:636-47.

11. di Martino E, Tomlinson DC, Knowles MA. A Decade of FGF Receptor Research in Bladder Cancer: Past, Present, and Future Challenges. Adv Urol 2012;2012:429213.

12. Whitesell L, Lindquist SL. HSP90 and the chaperoning of cancer. Nat Rev Cancer 2005;5:761-72.

13. Solit DB, Rosen N. Hsp90: a novel target for cancer therapy. Curr Top Med Chem 2006;6:1205-14.

14. Trepel J, Mollapour M, Giaccone G, Neckers L. Targeting the dynamic HSP90 complex in cancer. Nat Rev Cancer 2010;10:537-49.

15. Taldone T, Gozman A, Maharaj R, Chiosis G. Targeting Hsp90: small-molecule inhibitors and their clinical development. Curr Opin Pharmacol 2008;8:370-4.

16. Neckers L, Workman P. Hsp90 molecular chaperone inhibitors: are we there yet? Clin Cancer Res 2012;18:64-76.

17. Ying W, Du Z, Sun L, Foley KP, Proia DA, Blackman RK, et al. Ganetespib, a unique triazolone-containing Hsp90 inhibitor, exhibits potent antitumor activity and a superior safety profile for cancer therapy. Mol Cancer Ther 2012;11:475-84.

18. Sang J, Acquaviva J, Friedland JC, Smith DL, Sequeira M, Zhang C, et al. Targeted inhibition of the molecular chaperone Hsp90 overcomes ALK inhibitor resistance in non-small cell lung cancer. Cancer Discov 2013;3:430-43.

19. Tibes R, Qiu Y, Lu Y, Hennessy B, Andreeff M, Mills GB, et al. Reverse phase protein array: validation of a novel proteomic technology and utility for analysis of primary leukemia specimens and hematopoietic stem cells. Mole Cancer Ther 2006;5:2512-21.

20. Guagnano V, Furet P, Spanka C, Bordas V, Le Douget M, Stamm C, et al. Discovery of 3-(2,6-dichloro-3,5-dimethoxy-phenyl)-1-{6-[4-(4-ethyl-piperazin-1-yl)-phenylamin o]-pyrimidin-4-yl}-1-methyl-urea (NVP-BGJ398), a potent and selective inhibitor of the fibroblast growth factor receptor family of receptor tyrosine kinase. J Med Chem 2011;54:7066-83.

21. Karkoulis PK, Stravopodis DJ, Margaritis LH, Voutsinas GE. 17-Allylamino-17-demethoxygeldanamycin induces downregulation of critical Hsp90 protein clients and results in cell cycle arrest and apoptosis of human urinary bladder cancer cells. BMC Cancer 2010;10:481.

22. Eccles SA, Massey A, Raynaud FI, Sharp SY, Box G, Valenti M, et al. NVP-AUY922: a novel heat shock protein 90 inhibitor active against xenograft tumor growth, angiogenesis, and metastasis. Cancer Res 2008;68:2850-60.

23. Strassburg CP, Kalthoff S, Ehmer U. Variability and function of family 1 uridine-5'-diphosphate glucuronosyltransferases (UGT1A). Crit Rev Clin Lab Sci 2008;45:485-530.

24. Gong QH, Cho JW, Huang T, Potter C, Gholami N, Basu NK, et al. Thirteen UDPglucuronosyltransferase genes are encoded at the human UGT1 gene complex locus. Pharmacogenetics 2001;11:357-68.

25. Whitesell L, Bagatell R, Falsey R. The stress response: implications for the clinical development of hsp90 inhibitors. Curr Cancer Drug Targets 2003;3:349-58.

26. Cummings J, Ethell BT, Jardine L, Boyd G, Macpherson JS, Burchell B, et al. Glucuronidation as a mechanism of intrinsic drug resistance in human colon cancer: reversal of resistance by food additives. Cancer Res 2003;63:8443-50.

27. Singh D, Chan JM, Zoppoli P, Niola F, Sullivan R, Castano A, et al. Transforming fusions of FGFR and TACC genes in human glioblastoma. Science 2012;337:1231-5.

28. Soda M, Choi YL, Enomoto M, Takada S, Yamashita Y, Ishikawa S, et al. Identification of the transforming EML4-ALK fusion gene in non-small-cell lung cancer. Nature 2007;448:561-6.

29. Choi YL, Takeuchi K, Soda M, Inamura K, Togashi Y, Hatano S, et al. Identification of novel isoforms of the EML4-ALK transforming gene in non-small cell lung cancer. Cancer Res 2008;68:4971-6.

30. Sawyers CL. Chronic myeloid leukemia. New Engl J Med 1999;340:1330-40.

31. Greulich H, Pollock PM. Targeting mutant fibroblast growth factor receptors in cancer. Trends Mol Med 2011;17:283-92.

32. Nakashima T, Ishii T, Tagaya H, Seike T, Nakagawa H, Kanda Y, et al. New molecular and biological mechanism of antitumor activities of KW-2478, a novel nonansamycin heat shock protein 90 inhibitor, in multiple myeloma cells. Clin Cancer Res 2010;16:2792-802.

33. Laederich MB, Degnin CR, Lunstrum GP, Holden P, Horton WA. Fibroblast growth factor receptor 3 (FGFR3) is a strong heat shock protein 90 (Hsp90) client: implications for therapeutic manipulation. J Biol Chem 2011;286:19597-604.

34. O'Hare T, Eide CA, Deininger MW. Bcr-Abl kinase domain mutations, drug resistance, and the road to a cure for chronic myeloid leukemia. Blood 2007;110:2242-9.

35. Katayama R, Khan TM, Benes C, Lifshits E, Ebi H, Rivera VM, et al. Therapeutic strategies to overcome crizotinib resistance in non-small cell lung cancers harboring the fusion oncogene EML4-ALK. Proc Natl Acad Sci USA 2011;108:7535-40.

36. Chen Z, Sasaki T, Tan X, Carretero J, Shimamura T, Li D, et al. Inhibition of ALK, PI3K/MEK, and HSP90 in murine lung adenocarcinoma induced by EML4-ALK fusion oncogene. Cancer Res 2010;70:9827-36.

37. Normant E, Paez G, West KA, Lim AR, Slocum KL, Tunkey C, et al. The Hsp90 inhibitor IPI-504 rapidly lowers EML4-ALK levels and induces tumor regression in ALK-driven NSCLC models. Oncogene 2011;30(22):2581-6.

38. Rothman N, Garcia-Closas M, Chatterjee N, Malats N, Wu X, Figueroa JD, et al. A multi-stage genome-wide association study of bladder cancer identifies multiple susceptibility loci. Nature Genet 2010;42:978-84.

39. Izumi K, Zheng Y, Hsu JW, Chang C, Miyamoto H. Androgen receptor signals regulate UDP-glucuronosyltransferases in the urinary bladder: a potential mechanism of androgen-induced bladder carcinogenesis. Mol Carcinog 2013;52:94-102.

40. Tang W, Fu YP, Figueroa JD, Malats N, Garcia-Closas M, Chatterjee N, et al. Mapping of the UGT1A locus identifies an uncommon coding variant that affects mRNA expression and protects from bladder cancer. Hum Mol Genet 2012;21:1918-30.

Table 1. *In vitro* cytotoxicity values of ganetespib in bladder cancer cell lines.

Cell line	Ganetespib IC_{50} (nM)	FGFR3 status
DSH1	6	WT
SW-1710	6	WT
T24	7	WT
RT112	9	*FGFR3-TACC3*
639-V	10	R248C
SCaBER	10	WT
BFTC	17	WT
J82	18	K652E
HT-1376	21	WT
647-V	27	WT
UM-UC3	33	WT
LB831-BLC	34	WT
KU-19-19	36	WT
97-7	38	S249C
5637	44	WT
HT-1197	53	WT
MGH-U3	53	Y375C
TCCSUP	142	WT
RT4	1733	*FGFR3-TACC3*
SW780	3451	*FGFR3-BAIAP2L1*

Table 2. Fold-changes in protein expression following ganetespib treatment in RT112 bladder cancer cells using reverse phase protein array analysis.

Cellular Target	Protein	Fold Change
Receptor Tyrosine Kinases	MET (pY1235)	-2.7
	HER2	-2.2
	HER2 (pY1248)	-2.2
	EGFR (pY1068)	-1.9
	HER3	-1.6
	EGFR	-1.5
AKT signaling	AKT (pS473)	-2.5
	AKT	-2.4
	GSK3-A/B (pS2/S9)	-1.8
	PDK1 (pS241)	-1.7
	GSK3-A/B	-1.5
	PDK1	-1.4
MAPK pathway	C-RAF	-1.8
	MAPK (pT202/Y204)	-1.5
	MEK1 (pS217/S221)	-1.4
	Src (pY527)	-1.4
	P90RSK (pT359/S363)	-1.4
Transcription factors	c-Myc	-2.5
	NF-κB p65 (pS536)	-2.3
mTOR pathway	S6 (pS235/S236)	-13.2
	S6 (pS240/S244)	-8.9
	P70S6K (pT389)	-4.7
	4E-BP1 (pS65)	-2.5
	mTOR (pS2448)	-2.2
	Tuberin	-2.2
	TSC1	-1.3
	PRAS40 (pT246)	-1.2
Cell cycle regulation	Rb (pS807/811)	-4.6
	Chk1	-3.2
	Cyclin B1	-1.9
	CDK1	-1.4
	p21	+1.4
	p27	+1.5
Stress response	HSP70/72	+3.0
	HSP90 alpha	+1.6
Apoptosis	Caspase 7 (cleaved D198)	+2.5
	BIM	+1.4

Figure legends

Figure 1. Cellular viability, apoptosis induction and pathway modulation in FGFR3-TACC3-expressing RT112 cells following ganetespib treatment. A, RT112 cells were treated with increasing concentrations of ganetespib or BGJ398 and viability assessed after 72 hours. B, RT112 cells were treated with graded concentrations of ganetespib, as indicated. Caspase 3/7 activity was measured at 24 hours and viability assessed at 72 hours post-treatment. RLU, relative luminescence units. C, RT112 cells were exposed to increasing concentrations of ganetespib, or BGJ398 at 100nM, for 24 hours. The expression levels of FGFR3-TACC3, phosphorylated FGFR3, ERK and AKT (p-FGFR, p-ERK, p-AKT) and BIM were determined by immunoblotting. GAPDH, glyceraldehyde-3-phosphate dehydrogenase. D, RT112 cells were treated with 200 nM ganetespib and harvested at 2, 4, 6 and 24 hours. Lysates were immunoblotted with the indicated antibodies. *V*, vehicle control at 24 hour time point.

Figure 2. Enhanced activity of ganetespib in combination with the pan-FGFR TKI inhibitor BGJ398 *in vitro* and *in vivo*. A, 72-hour combination viability assay with ganetespib and BGJ398 in RT112 cells. Percentages represent the amount of cell death observed at each of the corresponding dose levels. B, Mice bearing established RT112 xenografts (n=8 mice/group) were i.v. dosed with ganetespib (150 mg/kg) once weekly and BGJ398 (10 mg/kg) administered p.o. 7x/week, either alone or in combination. Percent T/C values are indicated to the right of each growth curve and the error bars are the SEM. * p= 0.0005. C, Mice bearing established RT112 xenografts (n=3 animals/group) were treated with either vehicle or ganetespib (150 mg/kg) for 24 and 72 hours. Tumors were resected and the relative expression levels of the indicated signaling proteins determined by phosphoprotein array analysis.

Figure 3. Differential sensitivity of RT4 bladder cancer cells to ansamycin- and resorcinol-based HSP90 inhibitors. A, RT4 cells were treated with increasing concentrations of ganetespib, AUY922, 17-AAG and 17-DMAG. Cell viability was assessed at 72 hours. B, RT4 cells were exposed to graded concentrations of 17-AAG or 17-DMAG, as indicated. The expression levels of wild type FGFR3 and the FGFR3-TACC3 fusion protein (higher MW bands) were determined by immunoblotting. *V*, vehicle control. C, RT4 cells were treated with 17-DMAG or 17-AAG, as indicated, for 24 hours. The levels of p-ERK, HER2, CDC2 and BIM were determined by immunoblotting. D, RT4 cells were exposed to graded concentrations of

ganetespib (0.1-1 μM) for 24 hours and lysates immunoblotted with the indicated antibodies. *V*, vehicle control.

Figure 4. Differential sensitivity of SW780 bladder cancer cells to ansamycin- and resorcinol-based HSP90 inhibitors. A, SW780 cells were treated with increasing concentrations of ganetespib, AUY922, 17-AAG and 17-DMAG. Cell viability was assessed at 72 hours. B, SW780 cells were treated with ganetespib (*gpib*), AUY922 or 17-AAG at the indicated concentrations for 24 hours. Lysates were immunoblotted with the indicated antibodies. *V*, vehicle control. C, SW780 cells were exposed to graded concentrations of ganetespib (0.1-5 μM) for 24 hours and lysates immunoblotted with the indicated antibodies.

Figure 5. High endogenous UGT1A enzyme expression in bladder cancer cells promotes the rapid metabolism of ganetespib. A, RT112 and SW780 cells were treated with graded concentrations of ganetespib or 17-DMAG (10-1000 nM) for 1 and 24 hours, as indicated. Intracellular drug concentrations of the respective HSP90 inhibitors are plotted as a function of dose and time. B, RT112 and SW780 cells were cultured in 1 μM ganetespib. Cellular lysates were prepared and culture media collected at 15 minutes, 1, 4, 8, and 24 hours. The total intracellular concentration of ganetespib and its glucuronidated metabolites (*glu-ganetespib*), as well as drug concentrations in the media, were determined by LC-MS/MS. C, Cellular lysates prepared from SW780, RT4, RT112 and 97-7 bladder cancer cell lines were immunoblotted for UGT1A enzyme expression. D, Scatter plot of differential UGT1A gene expression between the SW780 and RT112 cell lines following PCR analysis. The axes of the scatter plot are the relative mRNA expression levels; outer parallel lines indicate a fourfold-change in gene expression threshold. Each spot represents an individual UGT1A gene family member, as indicated. E, Cellular lysates prepared from UGT1A10- and 1A9-transfected 293T cells (positive controls), SW780, RT4, and RT112 bladder cancer cell lines were immunoblotted for UGT1A9 and UGT1A10 enzyme expression.

Figure 6. Inhibition of UGT1A activity by RNA interference or competitive inhibition overcomes ganetespib resistance in SW780 cells. A, SW780 cells were transfected with non-targeting control or UGT1A7,8,9,10 siRNA for 72 hours. Cultures were treated with graded concentrations of ganetespib as shown for 24 hours. Lysates were immunoblotted with the indicated antibodies. B, SW780 cells were

treated with vehicle, ganetespib (0.5 μM), or propofol (100 μM or 300 μM), either alone or in combination, for 24 hours. Lysates were immunoblotted with the indicated antibodies.

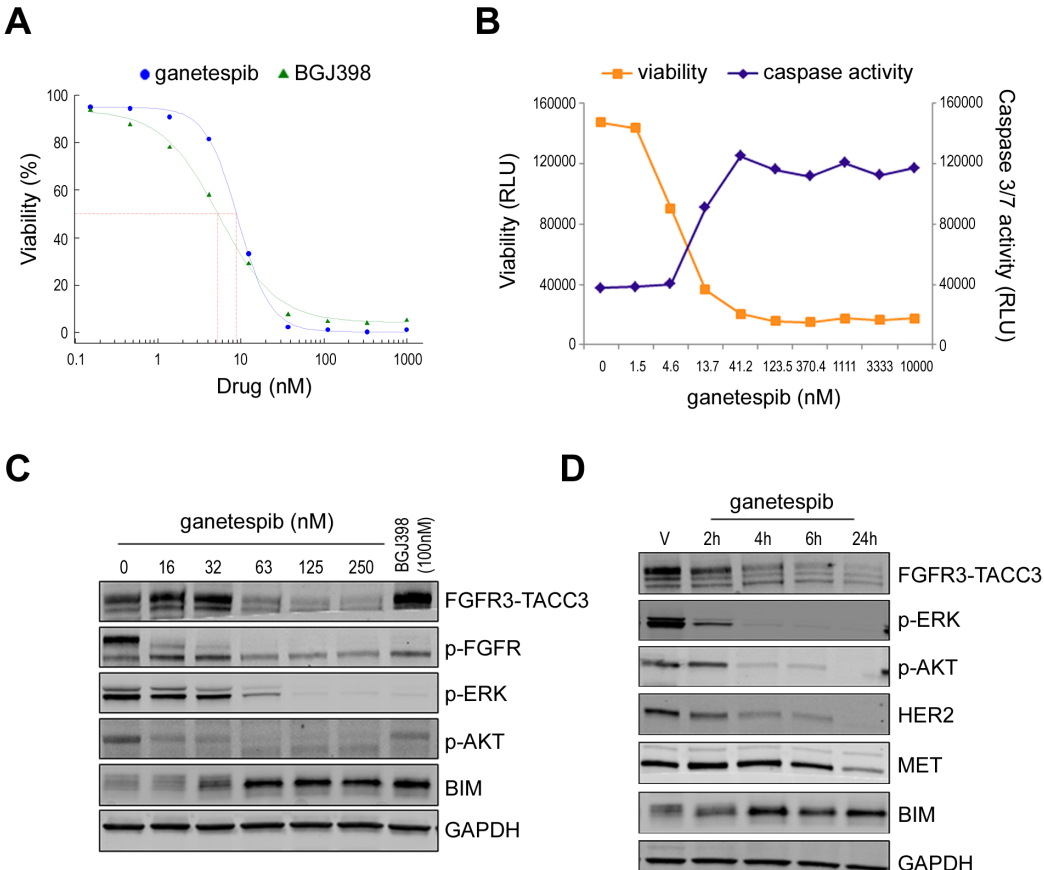
A
ganetespib
BGJ398
Viability (%)
Drug (nM)
B
viability
caspase activity
Viability (RLU)
Caspase 3/7 activity (RLU)
ganetespib (nM)
C
ganetespib (nM)
BGJ398 (100nM)
FGFR3-TACC3
p-FGFR
p-ERK
p-AKT
BIM
GAPDH
D
ganetespib
FGFR3-TACC3
p-ERK
p-AKT
HER2
MET
BIM
GAPDH

Figure 1

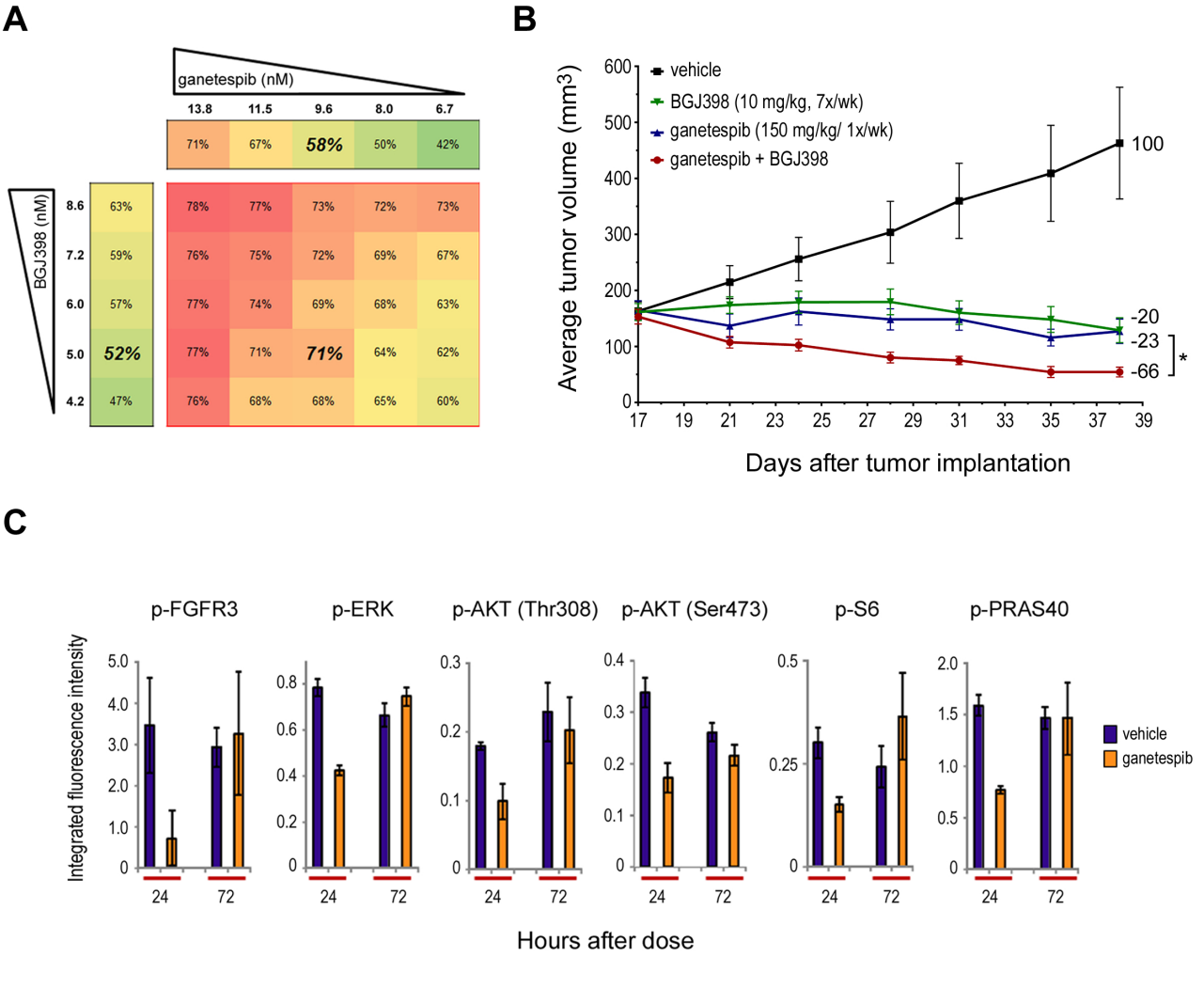
A
ganetespib (nM)
13.8
11.5
9.6
8.0
6.7
71%
67%
58%
50%
42%
BGJ398 (nM)
8.6
7.2
6.0
5.0
4.2
63%
59%
57%
52%
47%
78%
77%
73%
72%
73%
76%
75%
72%
69%
67%
77%
74%
69%
68%
63%
77%
71%
71%
64%
62%
76%
68%
68%
65%
60%
B
vehicle
BGJ398 (10 mg/kg, 7x/wk)
ganetespib (150 mg/kg/ 1x/wk)
ganetespib + BGJ398
Average tumor volume (mm3)
Days after tumor implantation
100
-20
-23
-66
*
C
p-FGFR3
p-ERK
p-AKT (Thr308)
p-AKT (Ser473)
p-S6
p-PRAS40
Integrated fluorescence intensity
Hours after dose
vehicle
ganetespib

Figure 2

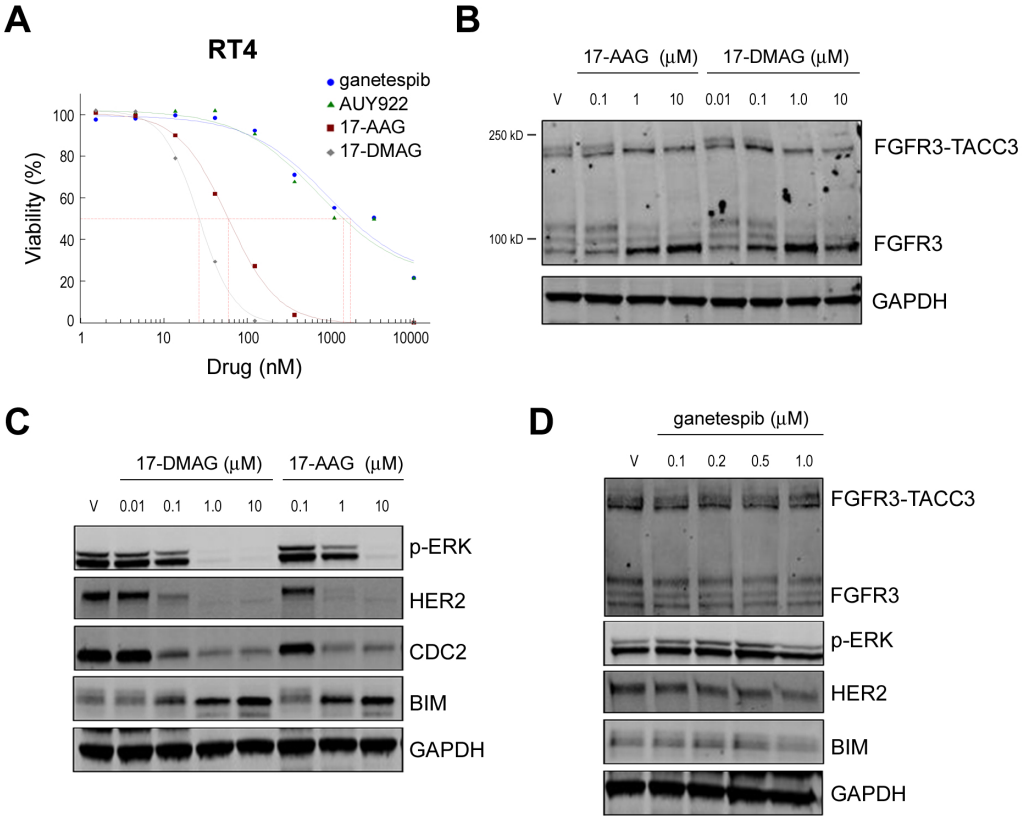
A
RT4
ganetespib
AUY922
17-AAG
17-DMAG
Viability (%)
Drug (nM)
B
17-AAG (μM)
17-DMAG (μM)
V 0.1 1 10 0.01 0.1 1.0 10
250 kD
100 kD
FGFR3-TACC3
FGFR3
GAPDH
C
17-DMAG (μM)
17-AAG (μM)
V 0.01 0.1 1.0 10 0.1 1 10
p-ERK
HER2
CDC2
BIM
GAPDH
D
ganetespib (μM)
V 0.1 0.2 0.5 1.0
FGFR3-TACC3
FGFR3
p-ERK
HER2
BIM
GAPDH

Figure 3

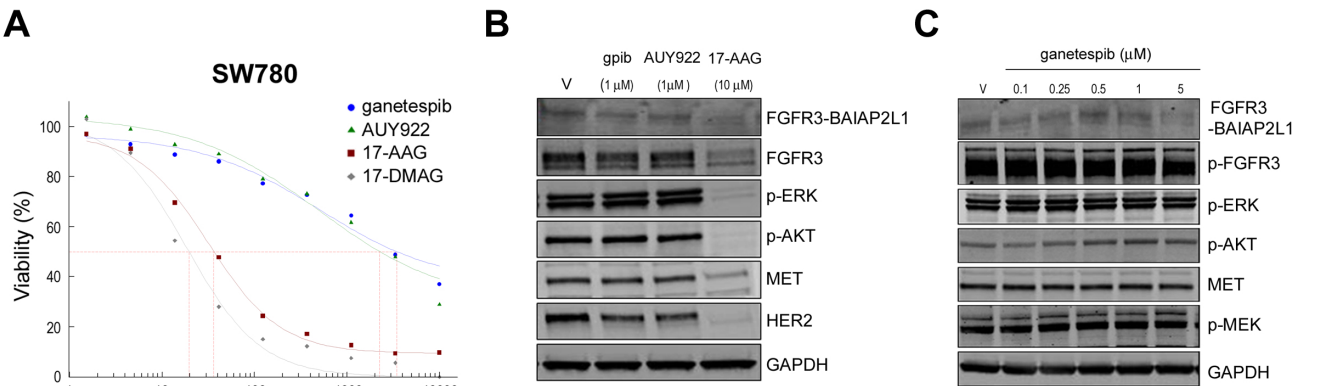
A
SW780
ganetespib
AUY922
17-AAG
17-DMAG
Viability (%)
Drug (nM)
B
V
gpib (1 μM)
AUY922 (1μM)
17-AAG (10 μM)
FGFR3-BAIAP2L1
FGFR3
p-ERK
p-AKT
MET
HER2
GAPDH
C
ganetespib (μM)
V
0.1
0.25
0.5
1
5
FGFR3 -BAIAP2L1
p-FGFR3
p-ERK
p-AKT
MET
p-MEK
GAPDH

Figure 4

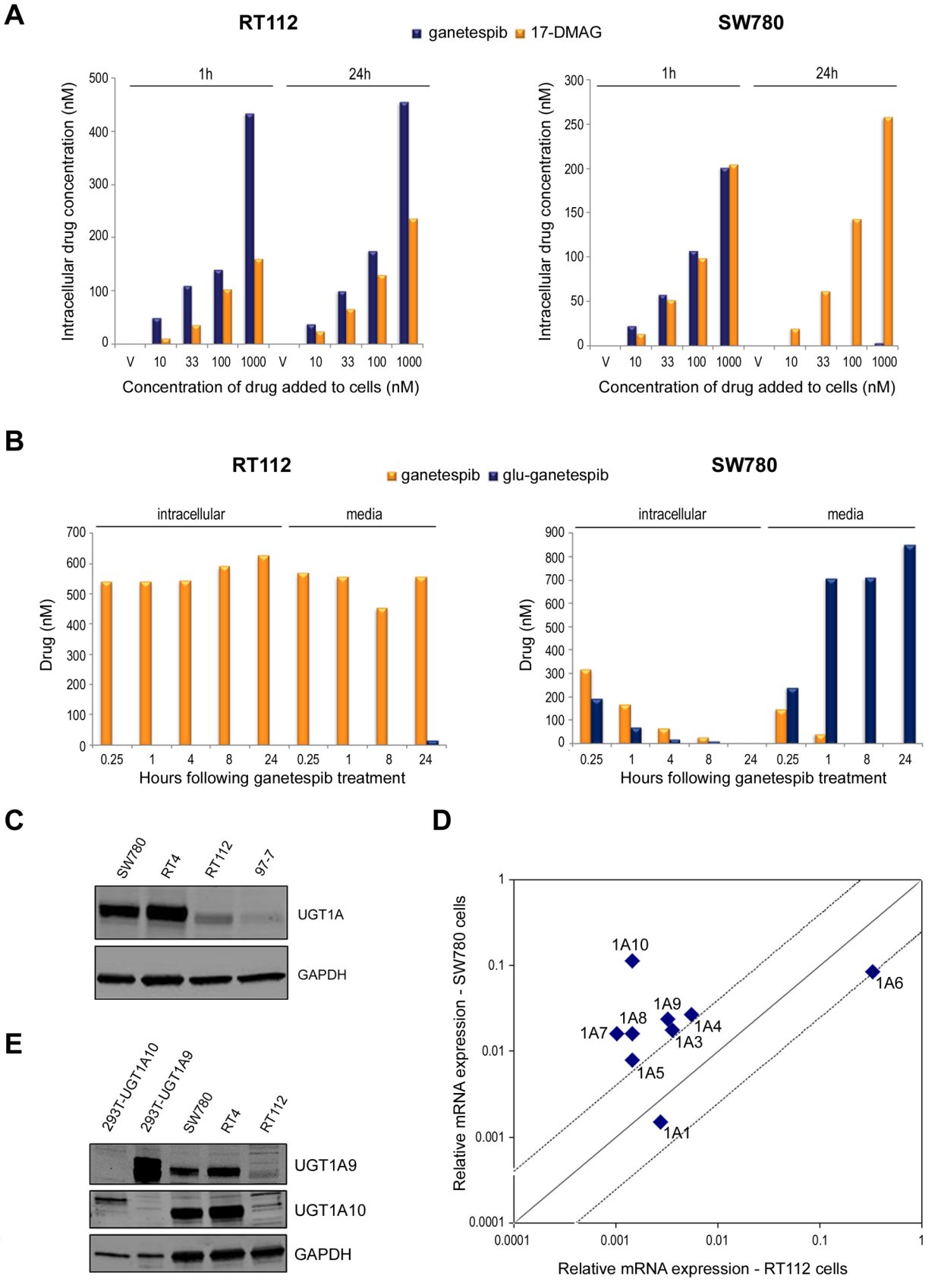
A
RT112
ganetespib
17-DMAG
SW780
1h
24h
Intracellular drug concentration (nM)
Concentration of drug added to cells (nM)
V
10
33
100
1000
B
RT112
ganetespib
glu-ganetespib
SW780
intracellular
media
Drug (nM)
Hours following ganetespib treatment
0.25
1
4
8
24
C
SW780
RT4
RT112
97-7
UGT1A
GAPDH
D
Relative mRNA expression - SW780 cells
Relative mRNA expression - RT112 cells
1A10
1A6
1A9
1A8
1A4
1A7
1A3
1A5
1A1
E
293T-UGT1A10
293T-UGT1A9
SW780
RT4
RT112
UGT1A9
UGT1A10
GAPDH

Figure 5

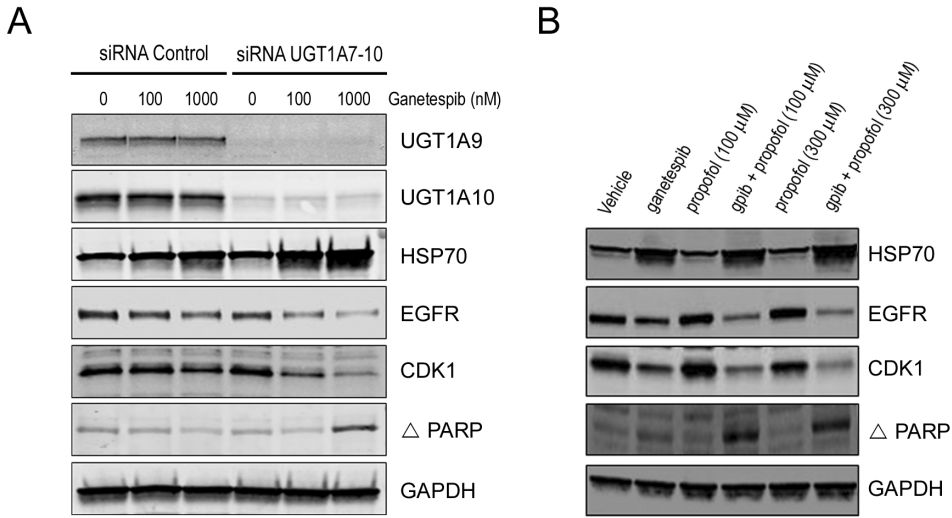
A
siRNA Control
siRNA UGT1A7-10
0
100
1000
0
100
1000
Ganetespib (nM)
UGT1A9
UGT1A10
HSP70
EGFR
CDK1
△ PARP
GAPDH
B
Vehicle
ganetespib
propofol (100 μM)
gpib + propofol (100 μM)
propofol (300 μM)
gpib + propofol (300 μM)
HSP70
EGFR
CDK1
△ PARP
GAPDH

Figure 6